

SeparaFill: Two generators connected mural image restoration based on generative adversarial network with skip connect

Yinghua Shen

Communication University of China

Zilu Li (✉ zilulee@cuc.edu.cn)

Communication University of China

Jinghua Li

Communication University of China

Jin Zheng

Communication University of China

Chaohui Lv

Communication University of China

Research Article

Keywords: SeparaFill, contour restoration generator, the content completion network, mural restoration

Posted Date: May 13th, 2022

DOI: <https://doi.org/10.21203/rs.3.rs-1638201/v1>

License:  This work is licensed under a Creative Commons Attribution 4.0 International License.

[Read Full License](#)

1 **SeparaFill: Two generators connected mural image restoration**
2 **based on generative adversarial network with skip connect**

3 **Yinghua Shen¹, Zilu Li^{1*}, Jinghua Li¹, Jin Zheng¹ and Chaohui Lv¹**

4 ¹Communication University of China, School of Information and Communication Engineering,

5 Digital Media Technology, Chaoyang District, Beijing, China, 100000

6 ***Correspondence:**Zilu Li, E-mail: zilulee@cuc.edu.cn

7 **Abstract**

8 Murals are the important components of culture and arts of Dunhuang. Unhappily, these murals
9 have been ruined or are being ruined by some diseases such as cracking, hollowing, falling off,
10 getting mildewed, dirt, and so on. Due to a lack of a standard mural datasets, Dunhuang mural
11 datasets are created by ourselves. Meanwhile, our proposed network architecture SeparaFill which
12 is connected two generators based on U-Net. First, the contour restoration generator network is
13 used to repair contour lines. Then, the color mural image is repaired by the content completion
14 network with help of the repaired contour. Next, global and local discriminant networks are applied
15 to determine whether the repaired mural image is authentic in terms of both the modified and
16 unmodified areas. Compared with existing mural restoration algorithms, the proposed method
17 increases the peak signal-to-noise ratio (PNSR) and increases the structural similarity (SSIM).
18 SeparaFill shows good performance in restoring the line structure of the damaged mural images
19 and retaining the contour information of the mural images.

20 **Keywords:** SeparaFill, contour restoration generator, the content completion network, mural
21 restoration

22 **Introduction**

23 Dunhuang murals retain the authentic works of famous artists over thousands of years, which have
24 profound artistic, historical and cultural value. Due to the long-term impact of natural weathering
25 and human factors, these murals have undergone different kinds of disease, such as cracking,
26 falling off, hollowing, pulverization, fading, color changing, getting mildewed, smudging and
27 scratches, and so on. Therefore, there is an urgent need to restore the murals combined with the
28 environment and painting materials. Meanwhile, the manual restoration work of Dunhuang murals
29 is arduous and complex, requiring the joint efforts and support of multiple disciplines¹. The
30 development of image processing and deep learning technology have allowed virtual restoration
31 of mural images to become a research hot-spot.

32 The research for virtual restoration of mural images are divided into two main categories, including
33 the digital image restoration based on traditional algorithms and the restoration method based on
34 deep learning. Cao et al.², Liu et al.³, and Yin et al.⁴ improved the traditional algorithm to restore
35 the mural image. While Wang et al.⁵, Zhang et al.⁶, and Wen et al.⁷ proposed the improvement
36 algorithms of the Generative Adversarial Networks (GAN)⁸ based on the deep learning research.
37 Currently, most of the researches are based on the public datasets of natural images in the field of
38 deep learning images restoration, which can capture the potential statistical laws in natural images
39 through the learning of massive data. Dunhuang murals are meticulous heavy color painting with
40 extremely and complexly structures and are obviously different from the natural images restored
41 by self-similarity characteristics, while the structure of mural images are mainly determined by the
42 line drawing. Due to the complex content of murals, it is also difficult to distinguish the foreground

43 and background. So, it is very difficult to restore the mural image well using the original GAN
44 networks. As there is lack of public mural image datasets so far, it is essential to establish the mural
45 datasets based on the Dunhuang mural album.

46 The mural images are mainly subject to damage from a wide variety of causes, resulting in some
47 small scale of mural diseases and some large areas missing. These small missing areas such as
48 cracking, small falling off blocks and pulverization of the mural, tend to appear in clusters and the
49 areas intertwined with the complete areas. These large missing areas such as scratch and large
50 peeling, account for a significant portion of the information of the mural image, which seriously
51 affects the integrity of the mural. In order to take advantage of effective information of the image,
52 good results can also be obtained in large-scale image restoration, a two generators connected
53 image restoration networks (SeparaFill) is proposed according to the characteristics of mural
54 painting. This algorithm based on U-Net network⁹ restore the contour lines of the image first and
55 then restore the color areas inside the contour lines of the image. The improvements achieved by
56 the proposed method are mainly reflected in the following aspects: (1) skip connections are added
57 to the contour restoration network for feature channel fusion to realize the reuse of low-level
58 features and extract the high-level semantic features of the image by using Hierarchical Residual
59 Networks(Res2Net)¹⁰; (2) an accumulation feature extraction mechanism is proposed to realize
60 multi-level feature fusion under different resolutions in the content completion restoration
61 network, and self-attention mechanism is introduced to restore image details. (3) Because of the
62 small datasets, the Siamese Network idea of Meta learning is introduced to the discriminator
63 network, and the contrast loss function commonly used in the Siamese Network is introduced into
64 the discriminator optimization. Compared with other algorithms, this method has achieved better
65 performance.

66 The traditional Image restoration algorithms are the ill-posed problems of filling in the missing
67 pixels in digital images by interpolating from the prior information. Rudin et al.¹¹ proposed the
68 Total Variation (TV), which used the partial differential equation based on the principle of thermal
69 diffusion to carry out anisotropic diffusion to repair the damaged areas. Zhang et al.¹² replaced the
70 integer order differential in the TV model with fractional order and further considered the image
71 texture structure information to improve the accuracy of image restoration. The TV method
72 achieves good effects on small missing areas, but it is prone to the problems of error diffusion and
73 poor visual connectivity. The algorithm based on texture synthesis proposed by Criminisi et al.¹³
74 considered the continuity of texture and can solve the problem of poor visual connectivity of partial
75 differential equations to a certain extent. On the basis of the above algorithm, Liu et al.¹⁴ and Cao
76 et al.² improved the confidence of priority and the adaptive selection of template window size to
77 optimize the effect of image restoration and avoided the diffusion phenomenon caused by the
78 restoration.

79 With the continuous development of deep learning, deep neural networks have shown excellent
80 ability in the prior knowledge learning of massive data. GAN networks can generate non-existent
81 images through the learning of image features and become a research hotspot in the field of image
82 restoration. Yeh et al.¹⁵ proposed a semantic image restoration model with depth generation mode
83 by adopting the Deep Convolutional GAN (DCGAN) structure and using context-weighted loss to
84 search for the closest encoding of the corrupted image, which has good performance on restoring
85 images with the simple structure. Zhang et al.¹⁶ used a four step incremental generation networks
86 to restore the image under the square mask, but this restoration method cannot deal with the
87 irregular mask. Liu et al.¹⁷ proposed an image restoration method based on partial convolution
88 (Pconv) by using partial convolution with mask instead of full convolution filling and it can repair

89 the irregular holes of images. Guo et al.¹⁸ designed the network generator as a network block with
90 two parallel branches of low resolution and full resolution. Through the superposition of network
91 blocks, the mask area was gradually cleaned and reduce to zero. Yu et al.¹⁹, Nazeri et al.²⁰ and
92 Zamir et al.²¹ adopted two connected generators to restore the image. Yu et al.²² further proposed
93 gate convolution on the previously model and replaced the ordinary convolution in the generator
94 to make the mask update learnable. Xiong et al.²³ proposed a three-stage image restoration model
95 to distinguish the foreground and background, which was suitable for a single object or
96 architectural image with clear outline and was not operable for images with complex lines and rich
97 content for murals. Ronneberger et al.²⁴, Li et al.²⁵, Yang et al.²⁶, Jo et al.²⁷ and Liu et al.²⁸
98 introduced skip connections into the corresponding convolution layer of down sampling and up
99 sampling based on the U-Net networks model to transfer the feature information extracted by the
100 networks, so as to improve the utilization efficiency of the networks for low-level features and
101 refine the texture of image restoration.

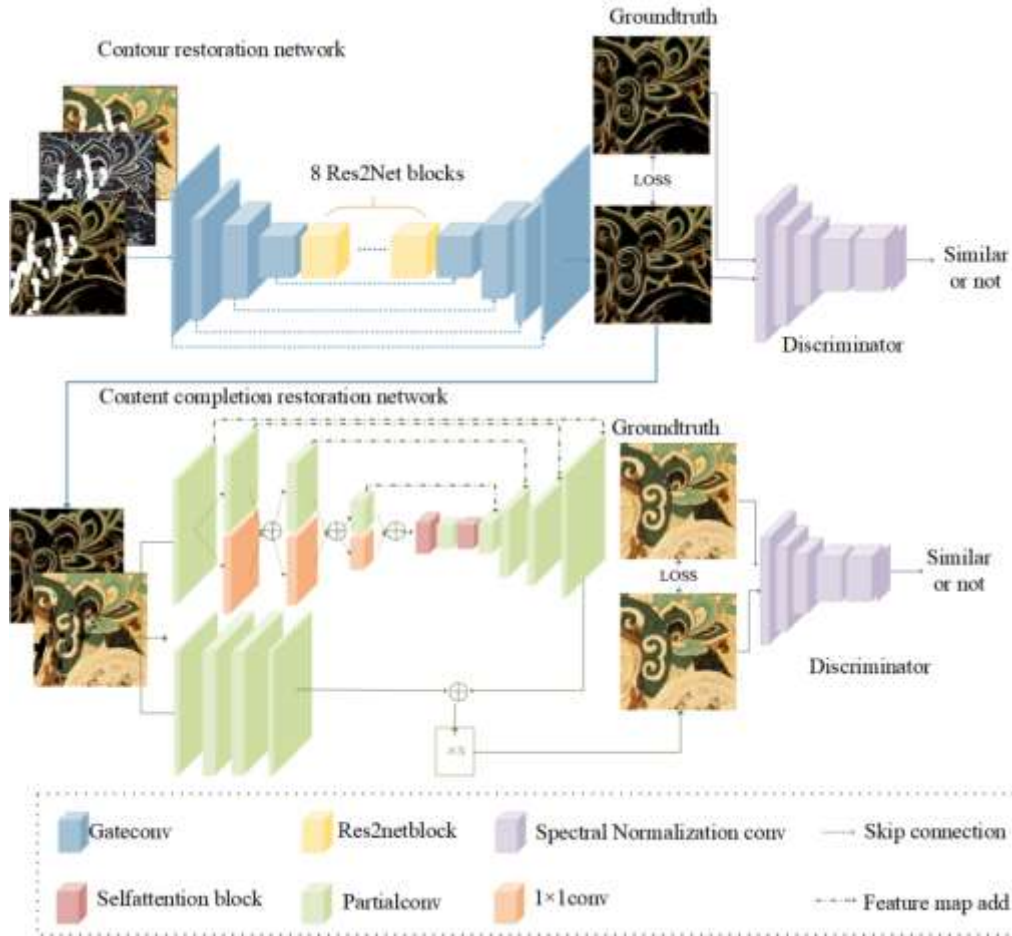
102 **Methods**

103 It is observed that the murals are dominated by contour lines through the analysis of the painting
104 characteristics of murals. Therefore, its pixels can be divided into contour line parts and color
105 block parts separated by contour line for a mural image. The contour line parts of the mural image
106 are composed of rich thin, narrow and continuous lines. Meanwhile, the color is relatively single,
107 which usually contains the dark colors such as black, brown and red. However the color block
108 parts contain rich color information. The size and shape depend on the contour line, but the gray
109 scale inside the color block is continuous and the texture information is simple. With the mural
110 image characteristics above, a two generators connected mural image restoration network based
111 on U-Net network architecture is proposed. This method restores the mural image contour and its

112 internal color blocks separately and reduces the difficulty of restoration. After two days of training,
113 the network can obtain the better restoration result compared with other algorithms.

114 The mural restoration network mainly consists of three parts: contour restoration generator
115 network, content completion restoration generator network, global and local discriminator
116 network.

117 The damaged image is obtained by multiplying the image with the mask, Let I_{gt} be ground truth
118 images, M be mask images, $x_{masked}^{(i)} = I_{gt} \odot M$ be the damaged image, $sketchgray^{(i)}$ is obtained by
119 the Holistically-nested Edge Detection (HED) algorithm²⁹, and the contour damaged image
120 $sketch_{masked}^{(i)} = x_{masked}^{(i)} \odot sketchgray^{(i)} \odot M$. Feed the damaged contour image and damaged image
121 into the contour restoration generator network, at the same time, Let $sobel^{(i)}$ as the edge image of
122 the damaged image via Sobel edge detection processing. Using the $x_{masked}^{(i)}$, $sketch_{masked}^{(i)}$ and
123 $sobel^{(i)}$ as input of contour restoration generator. Fill the contour recovery map $sketch_g^{(i)}$ into the
124 image's missing area, $x_{masked1}^{(i)} = sketch_g^{(i)} \odot (1-M) + x_{masked}^{(i)}$, the large missing block is further
125 divided into several small areas. The damaged contour image obtained by multiplying with the
126 mask is input into the contour repair generator network. At the same time, the sobel edge detection
127 processing is conducted on the damaged image to acquire the edge image, which is input to the
128 generator input end together with the damaged color image to assist the contour restoration. The
129 recovered contour is filled into the image to be repaired to further split the damaged areas of the
130 image. Meanwhile, the contour recovery map is also sent to the content completion restoration
131 generator in the second stage to guide the restoration of the image. The discriminator network of
132 contour restoration is as same as content completion restoration, which is composed of local
133 discriminator and global discriminator. The network framework is shown in Fig.1.



134

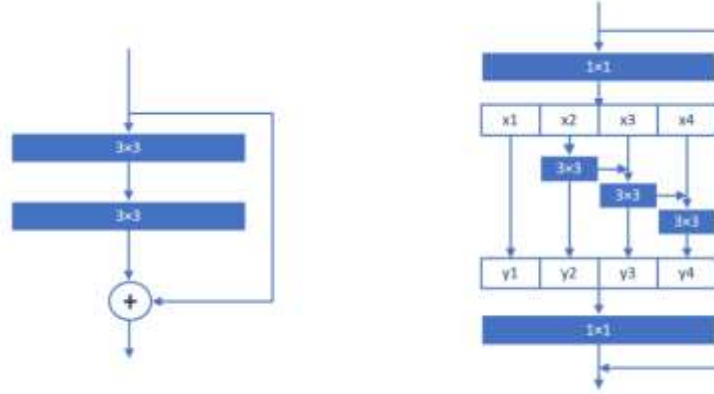
135

Fig.1 Our network framework

136 ***Contour restoration network***

137 The generator of the contour restoration network is improved on the Edgeconnect model²⁰. 9
 138 channels are put into the network, which include the damaged contour image of RGB (red, green,
 139 blue) three channels, the damaged image and the edge feature map extracted by Sobel edge
 140 detection. The input of the damaged image with the edge image together provide rich information
 141 for network and guide the contour restoration. The network consists of a down sampling
 142 convolution block contained a 5×5 convolution layer and three 3×3 convolution layers, 8 Res2Net
 143 blocks and a up sampling recovery resolution convolution block. Added skip connections between
 144 the corresponding layers of 4-layer down sampling convolution layers and up sampling

145 convolution layers of the contour restoration generator, which, reuses the low-layer edge features,
 146 and retains more dimensional information. So, the up sampling network of the generator can select
 147 between shallow features and deep features to enhance the robustness of the network. For the
 148 convolution in the shallow feature extraction network and the up-sampling convolution network,
 149 we use gate convolution to replace the ordinary convolution.



150
 151 **Fig. 2** (a) Residual block of Edgeconnect and (b) Residual block of Res2Net

152 The block of Res2Net used to replace the residual block structure in contour restoration network.
 153 Res2Net block modifies the structure of Residual Networks (ResNet) block³⁰ which is shown in
 154 Fig.2. Firstly, the input features are passed through a layer of 1×1 convolution, further divide the
 155 output features equally according to the number of channels, and fuse the segmented features in
 156 different channel blocks. The expression formula is as follows:

$$157 \quad y_i = \begin{cases} x_i & i = 1; \\ K_i(x_i + y_{i-1}) & 1 < i \leq s \end{cases}$$

158 (1)

159 Where x_i represents the number of equally divided blocks, s represents the number of equally
 160 divided blocks, y represents the output of convolution, and $K_i()$ represents 3×3 convolution. The
 161 residual structure of Res2Net retains the function of ResNet to avoid gradient disappearance and

162 gradient explosion, and realizes channel block multiplexing of the 3×3 convolution layer in the
163 ResNet block. This multi-scale channel fusion of input features can make the ability of feature
164 extraction stronger without add network parameters.

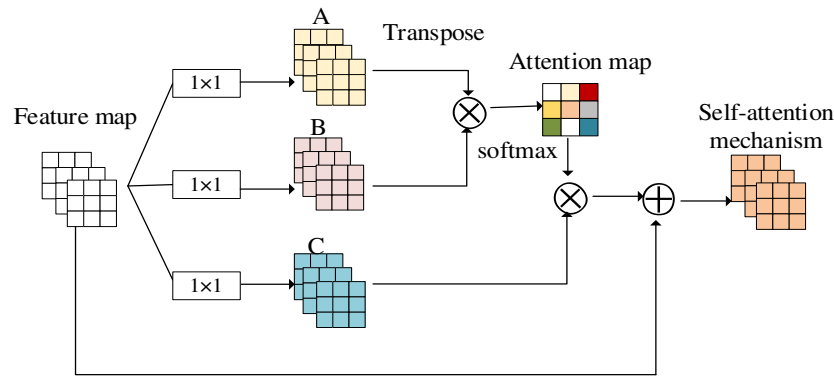
165 *Content completion restoration network*

166 The aim of the second stage is to complete the color blocks between the contour lines. The network
167 inputs are the contour map generated in the first stage and the corresponding damaged image after
168 repairing contour lines. The inpainting blocks include a U-shaped restore network branch and an
169 original resolution branch without down sampling, filling the missing area gradually and finely by
170 superimposing multiple blocks. The U-shaped restore branch consists of the 4 down sampling
171 convolution layers that the kernel is 3×3 with 2 step sizes, the feature extraction network with two
172 self-attention blocks, and up sampling layers of 3×3 convolution corresponding to the down
173 sampling layers. In order to reduce the network parameters and the memory occupation, so as to
174 increase the number of superimposed inpainting blocks for restoring delicately. The feature map
175 is directly added so that the feature map of each dimension will contains more characteristics.
176 Furthermore, an accumulation feature extraction mechanism is proposed, the feature map output
177 through each convolution layer is superimposed with the feature map output through the layer in
178 front, so as to realize multi-level feature fusion under different resolutions. The implementation
179 formula is as follows:

$$180 \quad y^l = \frac{y^l}{2^l} + \frac{1}{2^l} \sum_{i=1}^l 2^{i-1} y^i, \quad (2)$$

181 Where y^l represents the convolution fusion output of layer l , and y^i represents the fusion output
182 of convolution layer i . It can be seen from the formula that the superposition fusion mechanism
183 makes the features extracted by the fusion convolution layer accumulate the characteristics output

184 of all the convolution layers in front. Since the feature fusion of direct addition requires the same
 185 size of the input feature map, the feature map with different resolution is matched by reducing the
 186 resolution through 1×1 convolution layers.
 187 As the convolution kernel operates from the local region of the image and represents the local
 188 features, the influence of the global features on the current region becomes very small with the
 189 deepening of the convolution network. Self-attention mechanism³¹ can capture long-distance
 190 dependencies, namely paying attention to the global characteristics, so as to enlarge receptive
 191 fields of the network. After the feature accumulation layer, the self-attention mechanism is
 192 introduced to capture the overall features and detail features of the mural image, making the
 193 generated image more detailed.



194
 195 **Fig. 3** Structure of self-attention mechanism

196 The original resolution branch does not use down sampling in the process of transmitting and
 197 processing the input image information, so as to maintain the resolution of the original input
 198 information, assist in thinning the texture of the image restoration, and reuse the input information.
 199 Dilated convolutions are used in the content completion restoration network. The dilation is set as
 200 a loop of 1, 2 and 5 to increase the perception domain of the convolution. Since the large damaged
 201 area has divided into small pieces after the contour lines have been repaired in the first stage, the

202 difficulty of restoration becomes easier. Therefore, the partial convolutions with fewer parameters
 203 are used to update the mask and perform detailed restore through the superposition of modules.

204 ***Loss function***

205 The loss function in the contour inpainting phase is expressed as:

206
$$L_{s_G} = \lambda_{adv} L_{adv} + \lambda_{rec} L_{rec} + \lambda_{FM} L_{FM} , \quad (3)$$

207 Where L_{adv} is the adversarial loss based on the discriminator, L_{rec} is the L_1 reconstruction loss,

208 L_{FM} is the feature matching loss, and λ_{adv} , λ_{rec} and λ_{FM} are the weights of each loss respectively.

209 Generally, GAN obtains the optimal solution by optimizing the value function. The value function

210 is expressed as:

211
$$\min_G \max_D V(D, G) = E_{x \sim P_{data}(x)} [\log D(x)] + E_{i \sim P_{out}(i)} [\log(1 - D(G(i)))] , \quad (4)$$

212 Where x represents the input data, $P_{data}(x)$ represents the distribution of the real data, $P_{out}(i)$

213 represents the distribution of the image generated by the generator, D represents the discriminator,

214 the probability that the output input is the real data, and G represents the generator, which outputs

215 the generated image.

216 The goal of the discriminator is to maximize the value function. In view of the small mural datasets

217 and the characteristics of the discriminator structure, the contrast loss function commonly used in

218 the Siamese Network³² is introduced to transform the process of maximizing the value function of

219 the discriminator into the process of reducing the Euclidean distance between the truth image and

220 the generated image. The comparison loss function is expressed as follows:

221
$$d_loss = \frac{1}{2N} \sum_{n=1}^N y * d^2 + (1 - y) \max(m - d, 0)^2 , \quad (5)$$

222 Where y is the label of whether the input two samples (truth image and generator output image)

223 match or not, $y=1$ represents the similarity or matching of the two samples, $y=0$ represents the

224 mismatch, which $d = \|I_{gt} - I_{recover}\|_2$ represents the Euclidean distance between the ground truth
 225 image and the generated image, where $I_{recover}$ is the recovered image generated by the generator,
 226 I_{gt} is the input real image sample, m is the set threshold, which is set to 3 here.

227 The reconstruction loss is used to constrain the image pixel level restoration, so as to optimize the
 228 detail restore ability of the contour.

$$229 \quad L_{rec} = \|I_{recover} - I_{gt}\|_1 * \lambda_{rec} + \|I_{recover} \odot masks - I_{gt} \odot masks\|_1 * \lambda_{rec} , \quad (6)$$

230 Where $masks$ is the binary mask image, and \odot is the Hadamard product, used to calculate the
 231 global and local reconstruction losses for the generated image and the hole area under mask
 232 constraints respectively, λ_{rec} represents the weight value of the loss function.

233 The feature-matching loss is used to compare the feature maps in the intermediate layers of the
 234 discriminator. The feature-matching loss is expressed as follows:

$$235 \quad L_{FM} = E \left[\sum_{i=1}^L \frac{1}{N_i} \|D_1^{(i)}(I_{gt}) - D_1^{(i)}(I_{recover})\|_1 \right] * \lambda_{FM} , \quad (7)$$

236 Where L is the number of convolution layers of the discriminator, N_i is the number of characteristic
 237 diagrams of the activation layer of layer i , and $D_1^{(i)}$ is the activation number of layer of the
 238 discriminator. λ_{FM} is the regularization parameter.

239 The content restoration network needs to restore the texture of the image and maintain the semantic
 240 consistency between the restored image and the ground truth image. The loss function consists of
 241 confrontation loss, reconstruction loss, perception loss and structural similarity loss. The loss
 242 function is expressed as follows:

$$243 \quad L_G = \lambda_{adv} L_{adv} + \lambda_{rec} L_{rec} + \lambda_{SSIM} L_{MS-SSIM} + \lambda_{style} L_{style} , \quad (8)$$

244 The loss function and weight of the reconstruction loss L_{rec} and adversarial loss L_{adv} are the same
 245 as first part of contour restore. In order to better ensure that the texture and color of the image

246 restoration area fit the original mural, and make the style of the whole restored image consistent,
 247 the perceptual loss function³³ is introduced. The perceptual function is divided into content loss
 248 and style loss, compares the high-level abstract features through the VGG 19 pre-training model,
 249 the formula is as follows:

$$250 \quad I_{feat}^{\varphi,j}(\hat{y}, y) = \frac{1}{C_j H_j W_j} \left\| \varphi_j(\hat{y}) - \varphi_j(y) \right\|_2^2, \quad (9)$$

251 Where C_j , H_j and W_j represent the channel numbers, height and width of the characteristic graph
 252 respectively, j represents the j -th layer of the network, and φ represents the output after convolution network
 253 processing. Content loss let the generated image obtain better visual effect, but large loss weight will
 254 produce texture to image that does not conform to the original image, so it is necessary to reduce the weight
 255 of content loss in the later stage of training.

256 The multi-scale structure similarity loss function³⁴ is introduced. The combination of structural
 257 similarity loss and L1loss can balance the brightness and color of the image, thus making the
 258 restored image more detailed. The function expression is as follows:

$$259 \quad L_{MS-SSIM}(P) = 1 - MS-SSIM\left(\tilde{p}\right), \quad (12)$$

260 Where $MS-SSIM(\tilde{p})$ is SSIM calculation for images with different resolutions after scaling,
 261 which can obtain better results than simple SSIM loss.

262 **Training and testing procedures**

263 Limited by the small mural image datasets, when the parameter of batch size of training is set too
 264 large, which will affect the training results. So the parameter of batch size is set as 5, each of which
 265 batch has 3000 data, and the parameter of num_workers is set as 16, which is used to preload the
 266 batch data of the next iteration into memory. The specific algorithm steps are as follows:

267 **Table 1** Pseudocode of algorithm

Initialize the parameters of generator G, discriminators D1 and D2, iterations=n, batch_size=m, and the super parameter k=1 representing the steps of discriminator

for number of training iterations do

for k steps do

- The m real images $\{x^{(1)}, x^{(2)}, \dots, x^{(m)}\}$ were taken randomly from $P_{data}(x)$
- The m mask maps $\{M_1, M_2, \dots, M_m\}$ were taken in M_{mask} paired with the images
- via the HED networks to obtain contour $sketchgray^{(i)}$ from $x^{(i)}$
- $sketch^{(i)} = x^{(i)} \odot sketchgray^{(i)}$
- $x_{masked}^{(i)} = x^{(i)} \odot M$, $sketch_{masked}^{(i)} = sketch^{(i)} \odot M$
- $sketch_g^{(i)} = sketch^{(i)} \odot M + G_1(sketch^{(i)}, M) \odot (1 - M)$
- $x_{masked1}^{(i)} = sketch_g^{(i)} \odot (1 - M) + x_{masked}^{(i)}$
- Image inpainting $x_g^{(i)} = x_{masked1}^{(i)} \odot M + G_2(x_{masked1}^{(i)}, M) \odot (1 - M)$
- Calculate the restoration loss L_{dS} , L_d based on the input and restore samples
- Update the parameters of discriminators D1 and D2 through Adam optimization algorithm

end for

- Get m samples randomly from $P_{data}(x)$ and M_{mask} , constructing damaged images $x_{masked}^{(i)}$, $sketch_{masked}^{(i)}$, calculate the loss L_{dS} , L_d based on the input samples and restored samples generated by the network
- Update the parameters of discriminators D1 and D2 through Adam optimization algorithm

end for

268

269 **Results and discussion**

270 *Data source*

271 In this study, some clear and well preserved murals of characters in the Tang Dynasty from the
272 electronic scanning edition of *Dunhuang Mural Art* (all 10 volumes), *Chinese Dunhuang murals*
273 (all 11 volumes) and *Dunhuang Grottoes* (all 26 volumes) were used. After cleaning the image
274 data, eliminating duplicate mural images, 2175 original data images, consist of 172 images of the
275 early Tang Dynasty, 271 images of the prosperous Tang Dynasty, 859 images of the middle Tang
276 Dynasty, 743 images of the late Tang Dynasty and 130 images of the Five Dynasties were obtained,
277 and all of them were 512×512 in size. A total of 300 images were randomly selected from the
278 images of each dynasty as the test sets, and the remaining 1875 images as training sets. The datasets

279 is expanded by mirror operation, and then divided each original mural image into four small sub-
280 images (256×256) by horizontal and vertical segmentation. After that, a 15000 split training
281 datasets and a 2400 split test datasets were obtained and the size of each image was 256×256×3,
282 which contained rich mural feature elements such as the clothing, the texture, the face and the
283 decoration. The same number of images was randomly selected from the mask datasets to
284 correspond to the mural images one by one. The size of each mask image was 256×256×1. Mask
285 datasets imitated irregular damages such as cracking, falling off, pulverization, getting mildewed,
286 smudging and scratches in mural diseases. The damaged RGB image was obtained by multiplying
287 the mural image and the mask image.

288 *Experimental environment*

289 To verify the effectiveness of the proposed method, tests on mural image restoration were
290 conducted. The hardware environment in this experiment mainly consists of an Intel Xeon e5-2620
291 V4 @2.1GHZ with 128GB memory and four Nvidia GeForce GTX 1080 Ti graphics cards with
292 11GB memory. The software environment includes the JetBrains Pycharm compiler, running on a
293 Windows 10 system. The software was written in python 3.8, and Pytorch was used as the
294 framework for complete mural image restoration.

295 *Restoration of the randomly damaged murals*

296 In order to verify the effectiveness of the mural image restoration model proposed in this paper,
297 our network model are compared with Pconv¹⁷, Edgeconnect²⁰, FRRN¹⁸, RN³⁵ and RFR³⁶
298 networks on the test image datasets established in this paper. For the image restoration results of
299 different network models, peak signal-to-noise ratio (PSNR) and structural similarity (SSIM) are
300 used as the quantitative evaluation indices. The objective comparison of repair results is shown in

301 Table 2 and 3. Getting random mask from test mask datasets covers the test images to obtain the
 302 artificially damaged mural image, which is sent to the trained network to compare with the mural
 303 restore consequence. Otherwise, the running environment of all networks above is the same as our
 304 algorithm.

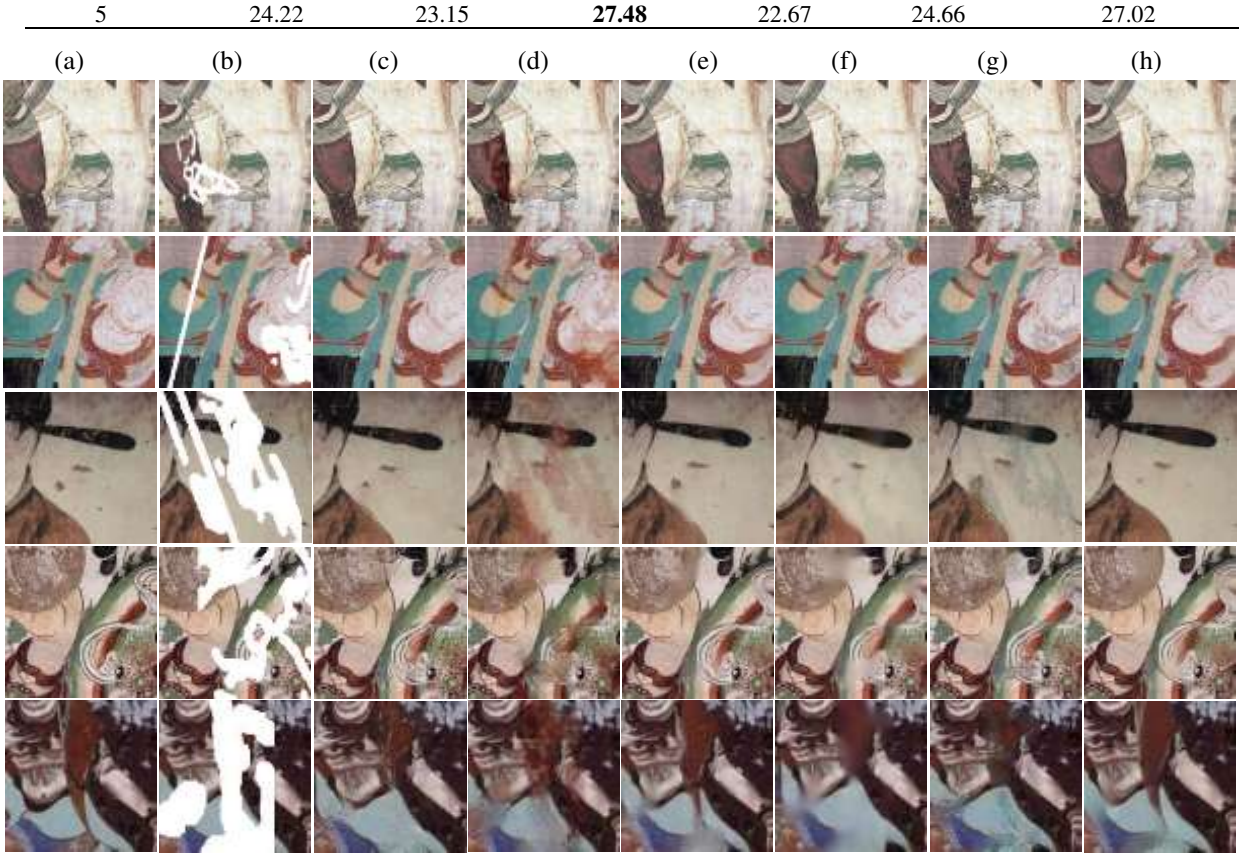
305 As can be seen from Fig.4, the restoration part of the algorithms in RN³⁵, Edgeconnect²⁰ and RFR³⁶
 306 is relatively fuzzy, and when the damaged area contains structural information, the original contour
 307 of the image cannot be well restored in algorithms Pconv¹⁷ and FRRN¹⁸, either. In this case, our
 308 network can not only obtain the prediction map with high PSNR and SSIM values, but also express
 309 the visual connectivity and structural consistency of the image well. With the increase of the degree
 310 of damage, the PSNR and SSIM of all 5 compared algorithms decrease significantly, problems
 311 such as incomplete inpainting, and image pixel error diffusion have appeared, however our
 312 algorithm can still maintain the contour integrity and continuity of mural image, such as ribbon,
 313 sphere, hat wing, shoulder of the characters in the painting, restoring its complete structure with
 314 less effective information of the image.

315 **Table 2** Comparison of SSIM value of each algorithm

Sample	Pconv	Edgeconnect	FRRN	RN	RFR	SeparaFill(ours)
1	0.9556	0.9187	0.9769	0.9322	0.9354	0.9788
2	0.9347	0.9113	0.9699	0.9434	0.9483	0.9677
3	0.7801	0.7904	0.9310	0.8774	0.8453	0.9234
4	0.7982	0.7509	0.8999	0.8108	0.8355	0.8826
5	0.8166	0.8135	0.9118	0.8291	0.8623	0.9067

316 **Table 3** Comparison of PSNR value of each algorithm

Sample	Pconv	Edgeconnect	FRRN	RN	RFR	SeparaFill(ours)
1	31.73	24.86	33.78	26.92	24.57	33.86
2	31.54	26.16	33.69	30.57	30.45	34.25
3	30.54	24.58	32.71	28.66	27.52	33.36
4	22.36	19.69	25.96	22.39	22.86	25.33



317
 318 **Fig.4** Comparison of large area damage restore results, (a) Ground truth, (b) Damaged image, (c) Pconv, (d)
 319 Edgeconnect, (e) FRRN, (f) RN, (g) RFR and (h) SeparaFill(ours)

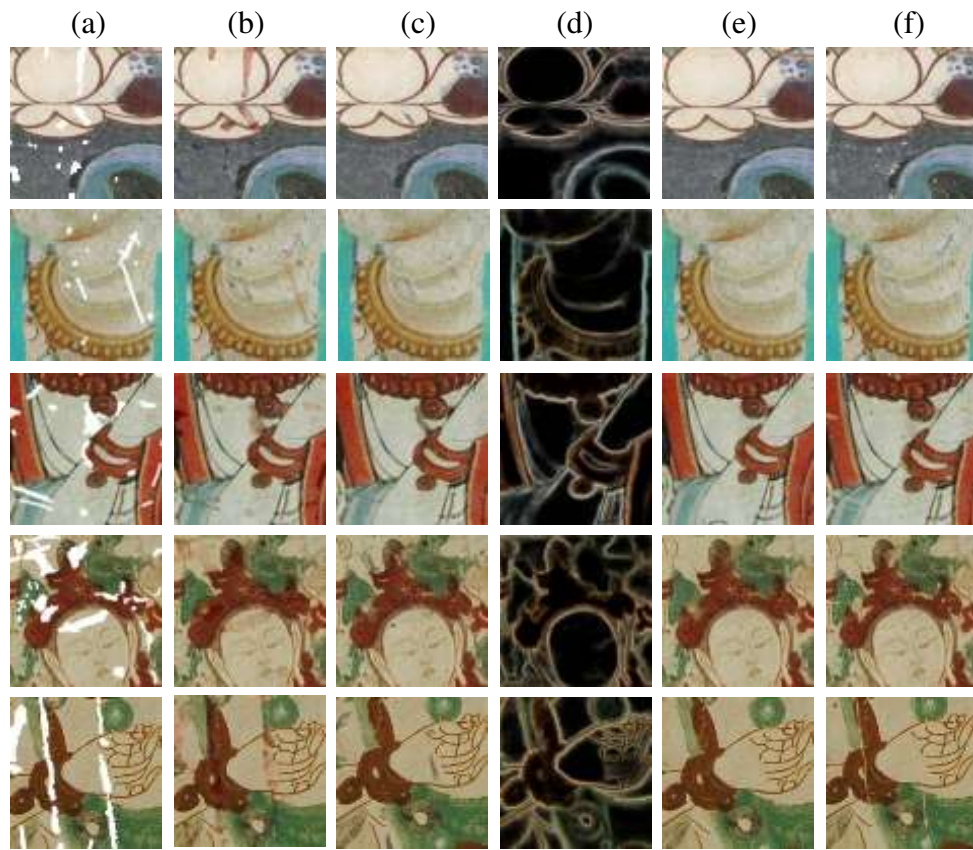
320 ***Restoration of the authentic damaged murals***

321 For the real damaged Dunhuang mural images, need to label and mark the real damaged area
 322 artificially, and the ground truth for these damaged historical relics disappeared many years
 323 ago. Therefore, we select some mural images and label the real damages with mask manually and
 324 compare our method with the algorithm in Ref [20] and [18], the objective comparison of repair
 325 results is shown in Table 4. It can be seen that the proposed method has significant advantages in
 326 objective evaluation in PSNR and SSIM indexes. As can be seen from Fig.5, our algorithm has a
 327 good and stable restore effect on distributed discrete damages, small pulverization, scratches,

328 cracks and other diseases, and keep the fill area consistent with the style and texture of the original
 329 image.

330 **Table 4** Comparison of SSIM value and PSNR value of each algorithm with large area damage restoration

Sample	Edgeconnect		FRRN		SeparaFill(ours)	
	PSNR	SSIM	PSNR	SSIM	PSNR	SSIM
1	25.19	0.8874	29.86	0.9457	30.65	0.9512
2	30.86	0.9540	33.72	0.9678	34.53	0.9714
3	25.69	0.8946	29.77	0.9566	31.76	0.9613
4	23.03	0.8327	26.98	0.9059	28.51	0.9206
5	26.11	0.8687	30.23	0.9342	32.36	0.9533



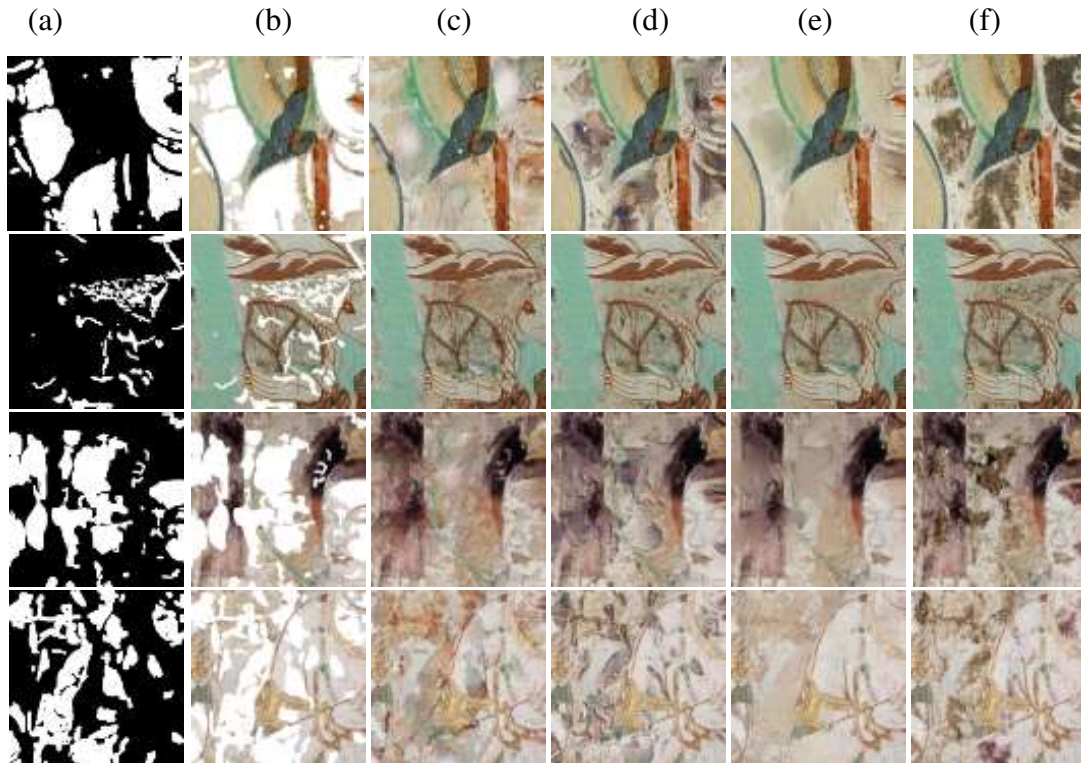
331
 332 **Fig.5** Comparison of small area real damage inpainting, (a) masked image, (b) Edgeconnect, (c) FRRN, (d) restored
 333 contour(ours), (e) SeparaFill(ours), (f) ground truth

334 For the large-area pulverization, falling off, fading and other diseases of murals, it is difficult to
 335 obtain realistic inpainting results because there is less effective information and it is very difficult
 336 to label the mask completely. As can be seen from Fig.6, our algorithm are more realistic and

337 natural than the results of the model Edgeconnect²⁰ and FRRN¹⁸, it can reduce the impact of the
 338 damaged area and restore the "original appearance" of murals as much as possible when the mask
 339 completely covers the damaged area.

340 **Table 5** Comparison of SSIM value and PSNR value of each algorithm with large area damage restoration

Sample	Edgeconnect		FRRN		SeparaFill(ours)	
	PSNR	SSIM	PSNR	SSIM	PSNR	SSIM
1	24.14	0.8524	26.51	0.9128	26.49	0.9558
2	18.32	0.6138	20.49	0.7185	18.92	0.7010
3	19.44	0.5834	20.62	0.6989	20.13	0.7027
4	14.72	0.5490	18.69	0.6601	15.13	0.6295



341
 342 **Fig.6** Comparison of large area real damage inpainting, (a) manual mask,(b) masked image, (c) Edgeconnect, (d)
 343 FRRN, (e) SeparaFill(ours), (f) ground truth

344 Conclusions

345 According to the painting characteristics of Dunhuang murals, we proposed a two generators
 346 connected image restoration networks (SeparaFill) based on U-Net and an accumulation feature

347 extraction mechanism to reuse the low-level features of images effectively. Firstly, the contour of
348 the image is completed, and then the completed image contour is used to guide the restoration of
349 color mural image. Experimental results indicate that our algorithm is very effective and possesses
350 outstanding inpainting performance for both the objective comparisons and the visual
351 performance. Compared with recent algorithms, our algorithm is also performed well in the large-
352 scale damaged image restoration and complex texture structures.

353 However, the contour line extracted from mural image is not very distinct because the mural image
354 is extracted directly on the HED network trained by the mural datasets. When extracting the
355 contour line, there is no improvement of network and neither modify the parameters of network.

356 At the same time, the image source comes from the electronic scanning version of the mural album,
357 which has greatly influence on the quality of the mural image in the process of printing and
358 scanning. The pixel blocks at the edge of the damaged area are badly jagged, so it is very difficult
359 to cover them one by one during the manual mask labels. Due to the above problems, the inpainting
360 of some local details of line structures is not very ideal. In the future, we will search for high-
361 quality mural images to create datasets, and the contour extraction algorithm will be improved to
362 obtain the distinctly contour of mural images. For large damaged mural images, the interactive
363 manual assistance will be provided to restore line details and labeled more accurately to reduce the
364 adverse effects caused by inaccurate calibration.

365 **Abbreviations**

366 GAN: Generative adversarial network; ResNet: Residual Networks; Res2Net:: Hierarchical Residual
367 Networks; VGG :Visual Geometry Group Network.

368 **Availability of data and materials**

369 All data for analysis in this study are included within the article.

370 **Competing interests**

371 The authors declare that they have no competing interests

372 **Funding**

373 None.

374 **Authors' contributions**

375 All the authors contributed to the current work. S.YH and L.ZL devised the study plan and led the
376 writing of the article. L.JH and Z.J arranged the data of experiment. S.YH and L.CH supervised
377 the entire process and provided constructive advice. All authors read and approved the final
378 manuscript.

379 **Acknowledgments**

380 None.

381 **Authors' information**

382 1School of Information and Communication Engineering, Communication University of China,
383 Beijing 100000, China

384 **References**

- 385 1. Fan JS. For the long-term existence of Dunhuang -Dunhuang Grotto protection exploration.
386 Dunhuang research.2004;111:35-9.
- 387 2. Cao JF et al. Repair of ancient temple view murals by local search algorithms for adaptive sample
388 blocks. Journal of Computer-aided Design and Graphs. 2019;31:112030-2037.

- 389 3. Liu YC. Study on Yunnan mural restoration based on the improved Criminisi algorithm. Dissertation.
390 Yunnan University, Yunnan, 2017.
- 391 4. Yin Y. Application of digital image repair technology in barley field rock painting repair. Dissertation.
392 Ningxia University, Ningxia, 2019.
- 393 5. Wang N, Wang W, Hu W, et al. Thangka Mural Inpainting Based on Multi-scale Adaptive Partial
394 Convolution and Stroke-like Mask. IEEE Transactions on Image Processing, 2021;30:3720-3733.
- 395 6. Zhang MF. Computer-aided Mural Restoration Study Based on generative Adversarial Network.
396 Dissertation. Northwest University, Shannxi,2019.
- 397 7. Wen LL, Xu D, Zhang X, et al. Some irregular partial repair method of ancient mural based on
398 generative model. Graphic Journal. 2019;5:925-931.
- 399 8. Goodfellow I. J, Pouget-Abadie J, Mirza M, et al. Generative Adversarial Networks. Advances in
400 Neural Information Processing Systems. 2014;3:2672-2680.
- 401 9. Ronneberger O, Fischer P, Brox T. U-Net: Convolutional Networks for Biomedical Image
402 Segmentation. Springer, Cham. 2015; doi:10.1007/978-3-319-24574-4_28.
- 403 10. Gao S, Cheng M. M, Zhao K, et al. Res2Net: A New Multi-scale Backbone Architecture. IEEE
404 Transactions on Pattern Analysis and Machine Intelligence, 2019;43:2652-662.
- 405 11. Rudin L. I, Osher S, Fatemi E. Nonlinear total variation based noise removal algorithms. Physica D
406 Nonlinear Phenomena. 1992; doi:10.1016/0167-2789(92)90242-F.
- 407 12. Zhang G, Yan Y. Image repair of a fractional TV model combining the texture structure. Chinese
408 graphic Journal. 2019;24:5700-713.
- 409 13. Criminisi A, Pérez P, Toyama K. Object Removal by Exemplar-Based Inpainting. IEEE Computer
410 Society Conference on Computer Vision and Pattern Recognition, 2003;doi:
411 10.1109/CVPR.2003.1211538.
- 412 14. Liu X. Image and video repair based on the hybrid Criminisi algorithm. Dissertation. Shandong
413 University, Shandong,2020.

- 414 15. Yeh R. A, Chen C, Lim T. Y, et al. Semantic Image Inpainting with Deep Generative Models. IEEE
415 Conference on Computer Vision and Pattern Recognition. 2017;1:6882-6890.
- 416 16. Zhang H, Hu Z, Luo C, et al. Semantic Image Inpainting with Progressive Generative Networks. acm
417 multimedia. 2018;1939-1947.
- 418 17. Liu G, Reda F. A, Shih K. J, et al. Image Inpainting for Irregular Holes Using Partial Convolutions.
419 European Conference on Computer Vision. 2018;doi:10.1145/3240508.3240625.
- 420 18. Guo Z, Chen Z, Yu T, et al. Progressive Image Inpainting with Full-Resolution Residual Network. in
421 Proceedings of the 27th ACM International Conference on Multimedia (MM '19).
422 2019;doi:10.1145/3343031.3351022.
- 423 19. Yu J, Lin Z, Yang J, et al. Generative Image Inpainting with Contextual Attention. CVF Conference
424 on Computer Vision and Pattern Recognition IEEE. 2018;2:5505-5514.
- 425 20. Nazeri K, Ng E, Joseph T, et al. EdgeConnect: Generative Image Inpainting with Adversarial Edge
426 Learning. ICCV Workshops. 2019; arXiv.1901.00212.
- 427 21. Zamir S. W, Arora A, Khan S, et al. Multi-Stage Progressive Image Restoration. Computer Vision
428 and Pattern Recognition IEEE. 2021;14821--14831.
- 429 22. Yu J, Lin Z, Yang J, et al. Free-Form Image Inpainting with Gated Convolution. International
430 Conference on Computer Vision. IEEE; 2019;4470-4479.
- 431 23. Xiong W, Yu J, Lin Z, et al. Foreground-Aware Image Inpainting. Computer Vision and Pattern
432 Recognition. IEEE;2019;1:5833-5841.
- 433 24. Ronneberger O, Fischer P, Brox T. U-Net: Convolutional Networks for Biomedical Image
434 Segmentation. International Conference on Medical Image Computing and Computer-Assisted
435 Intervention. Springer Vieweg. Berlin, Heidelberg;2015;doi:10.1007/978-3-662-54345-0_3.
- 436 25. Li H, Wang W, Guo L, Zhou L. Deep feature rearrangement image repair algorithm based on a dual-
437 transfer network. Journal of Huazhong University of Science and Technology (Natural Science
438 Edition).2021;49:774-781.

- 439 26. Yang H, Yu Y. Image repair using channel attention with hierarchical residual networks. Journal of
440 Computer-aided Design and Graphs.2021;33:5671-681.
- 441 27. Jo Y, Park J. SC-FEGAN: Face Editing Generative Adversarial Network with User's Sketch and
442 Color. International Conference on Computer Vision: ETRI;2019;1:1745-1753.
- 443 28. Liu H, Jiang B, Song Y, et al. Rethinking Image Inpainting via a Mutual Encoder-Decoder with
444 Feature Equalizations. European Conference on Computer Vision Lecture Notes in Computer
445 Science.Springer. Cham. 2020;12347:725-741.
- 446 29. Xie S, Tu Z. Holistically-Nested Edge Detection. IEEE International Conference on Computer Vision
447 (ICCV). 2015;doi:10.1109/ICCV.2015.164.
- 448 30. He K, Zhang X, Ren S, et al. Deep Residual Learning for Image Recognition. IEEE Conference on
449 Computer Vision and Pattern Recognition (CVPR). Piscataway: IEEE;2016;770-778.
- 450 31. Vaswani A, Shazeer N, Parmar N, et al. Attention Is All You Need. Advances in Neural Information
451 Processing Systems.2017;6000-6010.
- 452 32. Chopra S, Hadsell R, Lecun Y. Learning a similarity metric discriminatively, with application to face
453 verification. Computer Society Conference on Computer Vision and Pattern Recognition (CVPR'05).
454 Piscataway: IEEE;2005;1:539-546.
- 455 33. Johnson J, Alahi A, Fei-Fei L.Perceptual Losses for Real-Time Style Transfer and Super-Resolution.
456 European Conference on Computer Vision, Springer, Cham.2016;doi: 10.1007/978-3-319-46475-
457 6_43.
- 458 34. Zhao H, Gallo O, Frosio I, et al. Loss Functions for Neural Networks for Image Processing.
459 Computer Science. 2015.
- 460 35. Yu T, Guo Z, Jin X, et al. Region Normalization for Image Inpainting. In: the 34th AAAI
461 Conference.2019.p.12733-12740.
- 462 36. Li J, Wang N, Zhang L, et al. Recurrent Feature Reasoning for Image Inpainting. Conference on
463 Computer Vision and Pattern Recognition (CVPR).2020.p. 7757-7765.